

Supporting Information

Lewis Basic Sites Rich Metal - Organic Framework Featuring Hydrogen-Bonding Acetylene Nano-trap for Efficient C₂H₂/CO₂ Separation

Mengyue Lu,^[a] Zhiwei Zhao,^[a] Yuhao Tang,^[a] Yating Wang,^[a] Feifei Zhang,^{*[a]} Jinping Li,^[a, b] and Jiangfeng Yang^{*[a, b]}

a College of Chemistry and Chemical Engineering, Taiyuan University of Technology, Taiyuan 030024, Shanxi Province, China

b State Key Laboratory of Clean and Efficient Coal Utilization, Taiyuan 030024, Shanxi Province, China

*Corresponding author:

E-mail: zhangfeifei0096@link.tyut.edu.cn; yangjiangfeng@tyut.edu.cn;

Experimental Section

1. Materials

Nickel nitrate hexahydrate ($\text{Ni}(\text{NO}_3)_2 \cdot 6\text{H}_2\text{O}$, 99%) and 3,3'-bipyridine-5,5'-dicarboxylic acid (H_2L , 98%) were purchased from Jilin Chinese Academy of Sciences-Yanshen Technology Co., Ltd. Tetrafluoroboric acid (HBF_4 , 48%) was purchased from Shanghai Aladdin Biochemical Technology Co., Ltd. *N,N*-dimethylacetamide (DMA, 99%) and acetone (CH_3COCH_3 , 99%) were provided by Sinopharm Chemical Reagent Co., Ltd. The above reagents were used directly without further purification. The distilled water used in the experiment was made by our laboratory.

2. Synthesis of TUTJ-201Ni

Synthesis of TUTJ-201Ni. We placed 9.0 mL of DMA, 0.9 mL of H_2O , and 0.1 mL of HBF_4 (48 wt %) in a 20 mL glass vial containing $\text{Ni}(\text{NO}_3)_2 \cdot 3\text{H}_2\text{O}$ (90.0 mg, 0.37 mmol) and H_2L (30.0 mg, 0.12 mmol). The vial was sealed and placed in an oven preheated to 353 K. The solvothermal reaction took place at this temperature for 48 h. The products were collected by suction filtration and washed several times with fresh DMA and acetone.

3. Fitting of pure component isotherms

The single-component C_2H_2 and CO_2 adsorption isotherms of TYUT-201Ni were fitted using the dual-site Langmuir-Freundlich (DSLFF) model, and R^2 was greater than 0.9999.

$$q = q_1 \frac{b_1 P^{1/n_1}}{1 + b_1 P^{1/n_1}} + q_2 \frac{b_2 P^{1/n_2}}{1 + b_2 P^{1/n_2}} \quad (1)$$

Where q is the equilibrium adsorbed amount of an adsorbent (mmol/g); q_1 and q_2 are the saturation uptakes of site 1 and site 2 (mmol/g); b_1 and b_2 are the affinity coefficients of site 1 and site 2 (1/bar); n_1 and n_2 are the corresponding deviations from an ideal homogeneous surface.

4. Q_{st} calculation

The Q_{st} of TYUT-201Ni with C_2H_2 and CO_2 were calculated using the C_2H_2 , CO_2 single-component adsorption isotherms at 273 K and 298 K via the Clausius-Clapeyron equation.

$$\ln \frac{p_2}{p_1} = \frac{\Delta H}{R} \left(\frac{1}{T_1} - \frac{1}{T_2} \right) \quad (2)$$

In the above equation, P represents the pressure, the unit is bar, T is the temperature in K, and R is the gas constant (8.314).

5. IAST calculations of adsorption selectivity

The two-component gas selectivity calculation formula is defined as:

$$S_{ads} = \frac{q_1 / q_2}{p_1 / p_2} \quad (3)$$

Where, q_1 and q_2 are the absolute adsorption amounts of the components, and p_1 and p_2 are the partial pressures of the components in the gas mixture.

6. Computational method

We employed the Grand Canonical Monte Carlo (GCMC) method to simulate the adsorption density of CO₂ and C₂H₂ in MOFs. All molecular dynamics simulations were conducted using the LAMMPS software package¹. The UFF4MOF potential² was used to describe the MOF, while the GAFF potential³ was applied to CO₂ and C₂H₂ molecules, with atomic charges calculated using the AM1-BCC method. Intermolecular interactions were described using Lennard-Jones potentials and Coulombic forces. The time step was set to 1 fs. Adsorption was simulated at 300 K and 1 atm for a duration of 1 ns, with molecular insertion and deletion attempts every 0.1 ps. Trajectories were exported every 10 ps, and the average adsorption density was calculated from these trajectories.

Density Functional Theory (DFT) was used to calculate the adsorption energies of CO₂ and C₂H₂ in MOFs. All DFT calculations were performed using the VASP software package⁴. The Perdew-Burke-Ernzerhof (PBE) exchange-correlation functional within the Generalized Gradient Approximation (GGA) was selected. A plane-wave cutoff energy of 500 eV was set to ensure computational accuracy. Γ -point was used for k-point sampling. During geometry optimization, the force tolerance was set to 0.02 eV/Å, and the energy convergence criterion was 10⁻⁵ eV. The adsorption energy is calculated using the following formula.

$$E_{ads} = E_{MOF+molecular} - E_{MOF} - E_{molecular} \quad \backslash * \text{MERGEFORMAT (0.1)}$$

Supporting Tables and Figures

Table S1 Comparison of C₂H₂ and CO₂.

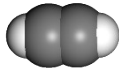
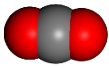
Gas molecules		
Boiling point (K)	189.3	194.7
Kinetic diameter (Å)	3.3	3.3
Molecular dimensions (Å ³)	3.32 × 3.34 × 5.70	3.18 × 3.33 × 5.36
Polarizability × 10 ²⁵ (cm ⁻³)	33.3-39.3	29.11
Dipole moment (e.s.u. cm)	0	0
Quadrupole moment × 10 ²⁶ (e.s.u. cm ²)	7.2	4.3
pKa	25	--

Table S2 Atomic content of TUTJ-201Ni.

Atomic	Ni	O	N
Content (%)	27.90	25.93	8.11

Note: The Ni content was determined using inductively coupled plasma optical emission spectrometry (ICP-OES) on an Agilent 5110 (OES) instrument. Other atomic content was evaluated by Elemental Analyzer.

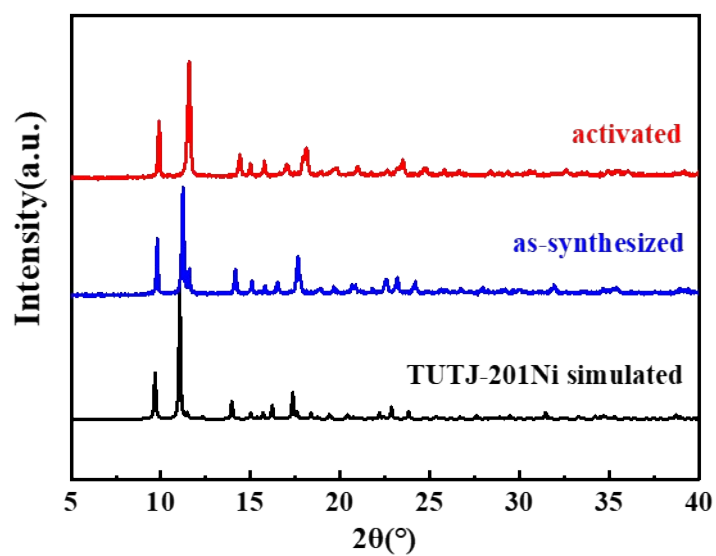


Figure S1. PXRD patterns of as-synthesized (blue) and activated TUTJ-201Ni (red) compared with the simulated XRD patterns from the structures of TUTJ-201Ni (black).

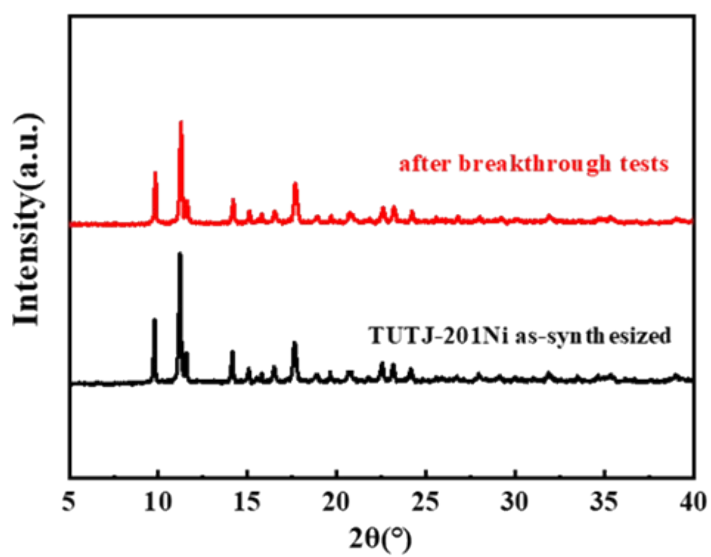


Figure S2. PXRD patterns of as-synthesized samples, and the sample after multiple breakthrough tests of TUTJ-201Ni.

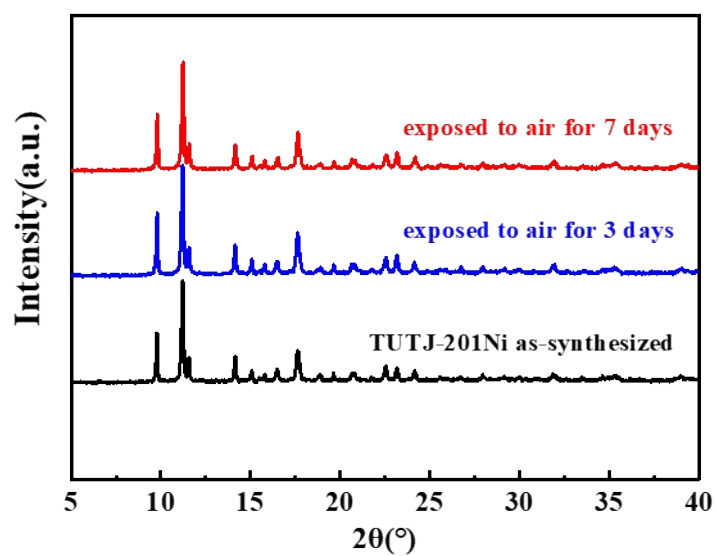


Figure S3. PXRD patterns of as-synthesized samples, the samples exposed to air for 3 days and 1 week of TUTJ-201Ni.

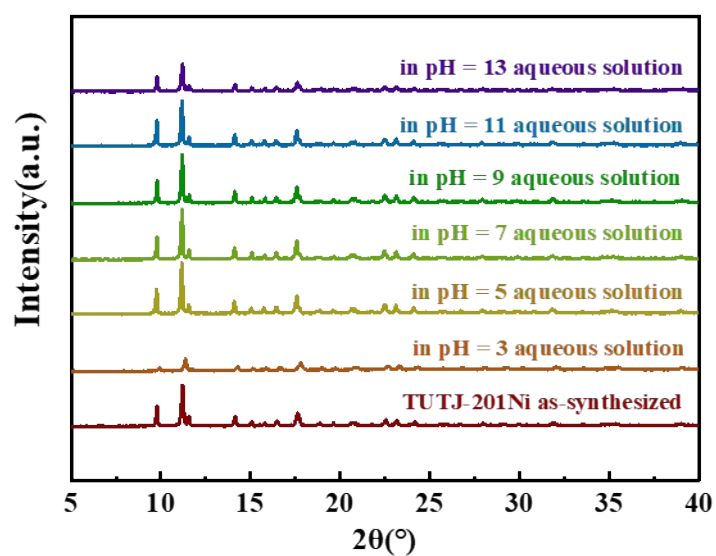


Figure S4. PXRD patterns of TUTJ-201Ni after treatment with pH =3, 5, 7, 9, 11, 13 aqueous solution for 3 days.

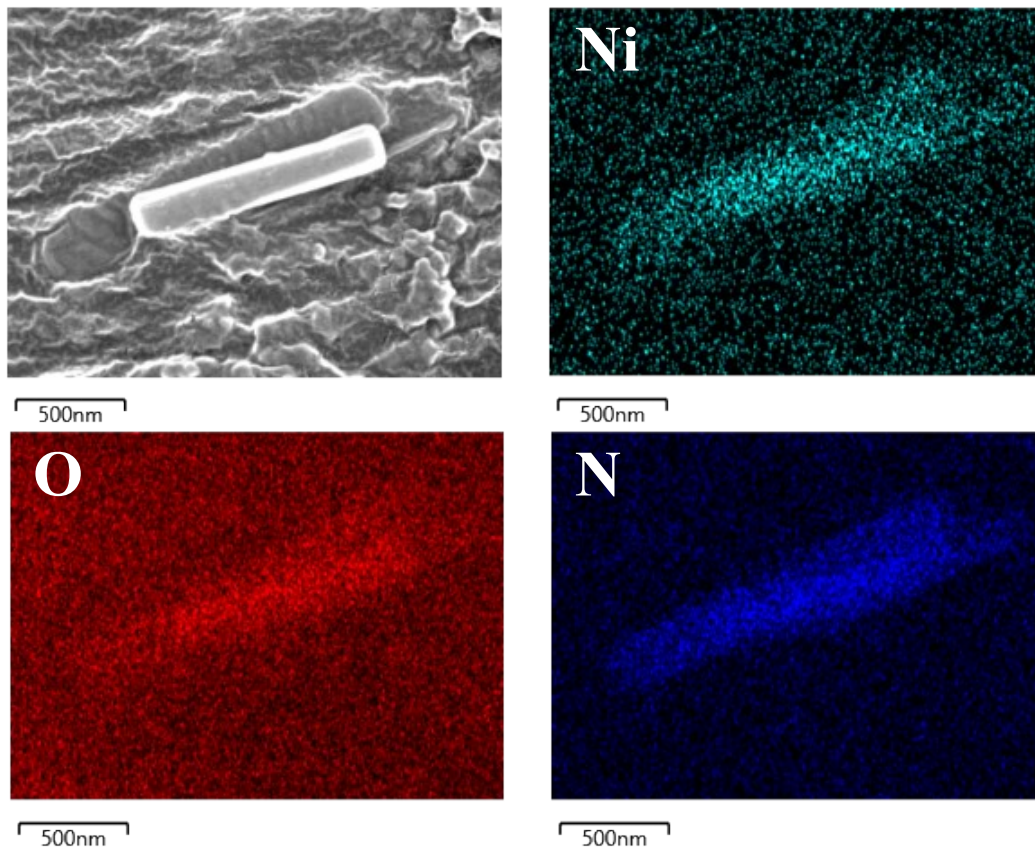


Figure S5. SEM and EDS images of as made TUTJ-201

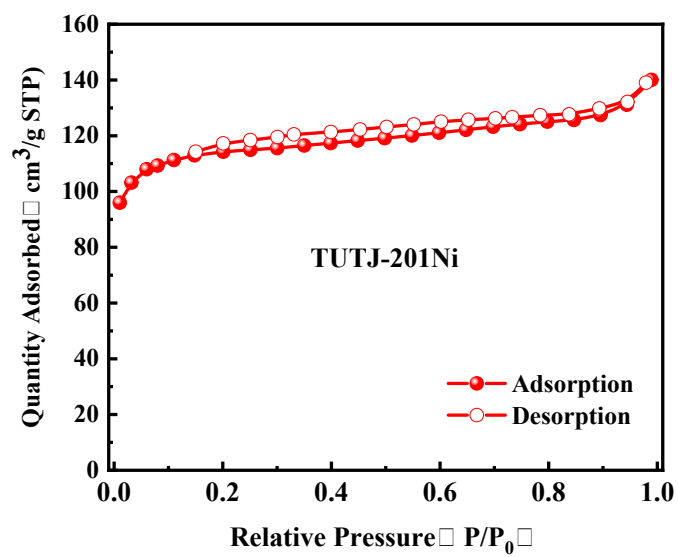


Figure S6. N₂ sorption isotherms obtained for TUTJ-201Ni at 77 K.

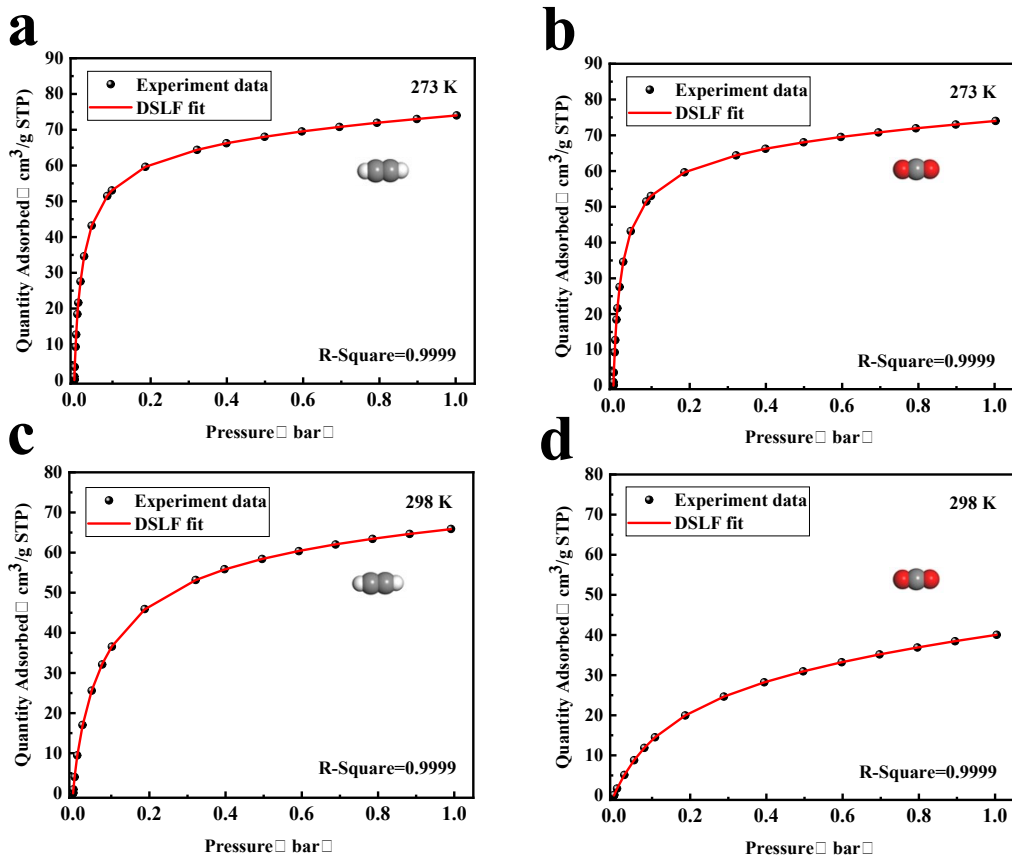


Figure S7. C_2H_2 and CO_2 adsorption isotherms at 273 and 298 K in TUTJ-201Ni with dual-site Langmuir-Freundlich model fits.

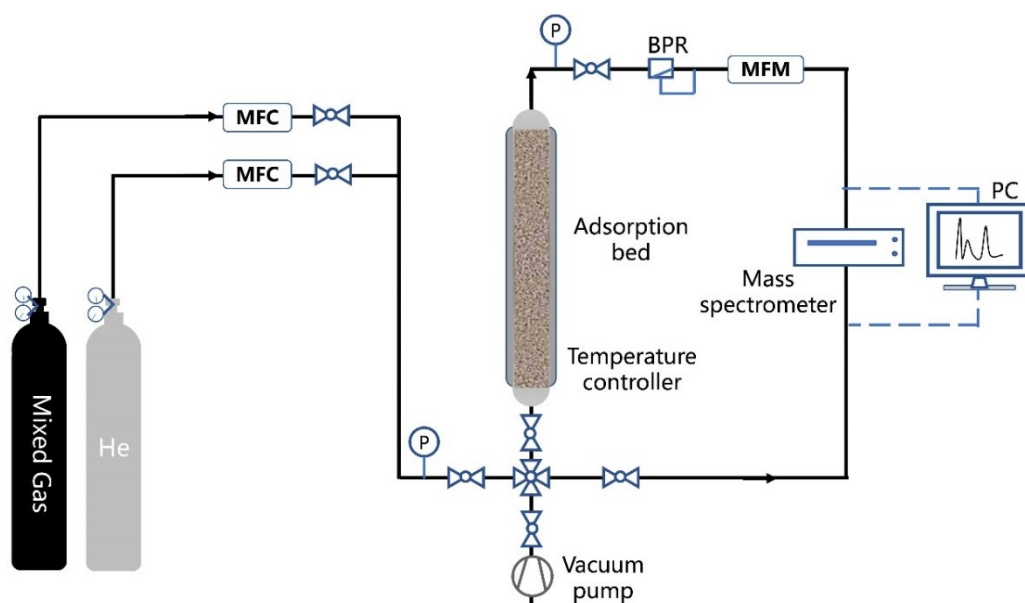


Figure S8. Schematic illustration of home-built rig for gas breakthrough experiment.

Table S3. Comparison of adsorptive separation properties of TUTJ-201Ni with the selected various porous materials reported in the literature.

Adsorbent	C₂H₂ uptake (cm³ g⁻¹)^a	CO₂ uptake (cm³ g⁻¹)^a	C₂H₂ <i>Q</i>_{st} (kJ mol⁻¹)^b	IAST Selectivity	Ref.
TUTJ-201Ni	55.3	40.1	34.66	7.0	This work
ATC-Cu	112.2	80.8	79.1	53.6	5
CuI@UiO-66-(COOH) ₂	52.4	17.2	74.5	185.0	6
NKMOF-1-Ni	61.0	51.1	60.3	22	7
UTSA-300a	68.9	3.25	57.6	21	8
SNNU-16	37.2	70.2	52.6	2	9
IPM-101	57.1	68.1	43.7	5.4	10
[Ni(dpip)]	83.6	14.3	41.7	2	11
TCuCl	67.2	44.8	41	5.3	12
[Ni ₃ (HCOO) ₆]	53.4	34.0	40.9	22.0	13
Cu(bpy)NP	50.7	25.1	40.8	343.8	14
SNNU-45	193.0	97.4	40.0	8.5	15
TIFSIX-2-Ni-i	94.3	101.7	40.0	6.1	16
UTSA-50	113.9	100.1	39.4	13.3	17
SIFSIX-Cu-TPA	185.0	107.0	39.1	5.3	18
NJU-Bai17	222.4	-	38.0	-	19
JXNU-18	55.2	31.5	37.4	2.81	20
JCM-1	75.0	38.0	36.9	13.7	21
Zn(adenine)(TCPE)	48.1	33.8	35.1	4.1	22
ZNU-9	177.9	100.8	33.1	10.3	23
NBU-7-Cl	34.3	25.0	33	3.3	24
FeNi-M'MOF	133.0	88.0	32.8	24	25
HKUST-1	201.0	-	30.4	-	26

FJU-6-TATB	110.0	58.0	29.0	5.3	27
ZNU-8	113.1	58.2	27.2	3.7	23
CAU-10-H	89.8	60.0	27.0	24.2	28
CAU-23	119.0	72.0	26.7	3.8	29
FJU-90	180.0	103.0	25.1	4.3	30
ZJU5	193.0	-	15.3	-	31

a. Gravimetric (mmol/g) at 298 K and 1 bar.

b. Calculated from the virial and Clausius-Clapeyron equation at low loading.

c. IAST selectivity for 50/50 (v/v) C₂H₂/CO₂ mixture at 1 bar.

References

1. A. P. Thompson, H. M. Aktulga, R. Berger, D. S. Bolintineanu, W. M. Brown, P. S. Crozier, P. J. in 't Veld, A. Kohlmeyer, S. G. Moore, T. D. Nguyen, R. Shan, M. J. Stevens, J. Tranchida, C. Trott and S. J. Plimpton, *Comput. Phys. Commun.*, 2022, **271**.
2. M. A. Addicoat, N. Vankova, I. F. Akter and T. Heine, *J. Chem. Theory Comput.*, 2014, **10**, 880-891.
3. J. Wang, R. M. Wolf, J. W. Caldwell, P. A. Kollman and D. A. Case, *J. Comput. Chem.*, 2004, **25**, 1157-1174.
4. G. Kresse and J. Hafner, *Physical Review B*, 1993, **47**, 558-561.
5. Z. Niu, X. Cui, T. Pham, G. Verma, P. C. Lan, C. Shan, H. Xing, K. A. Forrest, S. Suepaul, B. Space, A. Nafady, A. M. Al-Enizi and S. Ma, *Angew. Chem. Int. Ed.*, 2021, **60**, 5283-5288.
6. L. Zhang, K. Jiang, L. Yang, L. Li, E. Hu, L. Yang, K. Shao, H. Xing, Y. Cui, Y. Yang, B. Li, B. Chen and G. Qian, *Angew. Chem. Int. Ed.*, 2021, **60**, 15995-16002.
7. Y. L. Peng, T. Pham, P. Li, T. Wang, Y. Chen, K. J. Chen, K. A. Forrest, B. Space, P. Cheng, M. J. Zaworotko and Z. Zhang, *Angew. Chem. Int. Ed.*, 2018, **57**, 10971-10975.
8. R.-B. Lin, L. Li, H. Wu, H. Arman, B. Li, R.-G. Lin, W. Zhou and B. Chen, *J. Am. Chem. Soc.*, 2017, **139**, 8022-8028.
9. H.-P. Li, Z.-D. Dou, Y. Wang, Y. Y. Xue, Y. P. Li, M.-C. Hu, S.-N. Li, Y.-C. Jiang and Q.-G. Zhai, *Inorg. Chem.*, 2020, **59**, 16725-16736.
10. S. Sharma, S. Mukherjee, A. V. Desai, M. Vandichel, G. K. Dam, A. Jadhav, G. Kociok-Köhn, M. J. Zaworotko and S. K. Ghosh, *Chem. Mater.*, 2021, **33**, 5800-5808.
11. Y.-Z. Li, G.-D. Wang, L.-N. Ma, L. Hou, Y.-Y. Wang and Z. Zhu, *ACS Appl. Mater. Interfaces*, 2021, **13**, 4102-4109.
12. S. Mukherjee, Y. He, D. Franz, S. Q. Wang, W. R. Xian, A. A. Bezrukov, B. Space, Z. Xu, J. He and M. J. Zaworotko, *Chem. Eur. J*, 2020, **26**, 4923-4929.
13. L. Zhang, K. Jiang, J. Zhang, J. Pei, K. Shao, Y. Cui, Y. Yang, B. Li, B. Chen and G. Qian, *ACS Sustain. Chem. Eng.* 2018, **7**, 1667-1672.
14. Y. Liu, J. Liu, H. Xiong, J. Chen, S. Chen, Z. Zeng, S. Deng and J. Wang, *Nat. Commun.*, 2022, **13**, 5515.
15. Y. P. Li, Y. Wang, Y. Y. Xue, H. P. Li, Q. G. Zhai, S. N. Li, Y. C. Jiang, M. C. Hu and X. Bu, *Angew. Chem. Int. Ed.*, 2019, **58**, 13590-13595.
16. M. Jiang, X. Cui, L. Yang, Q. Yang, Z. Zhang, Y. Yang and H. Xing, *Chem. Eng. J* 2018, **352**, 803-810.
17. H. Xu, Y. He, Z. Zhang, S. Xiang, J. Cai, Y. Cui, Y. Yang, G. Qian and B. Chen, *J. Mater. Chem. A*, 2013, **1**, 77-81.
18. H. Li, C. Liu, C. Chen, Z. Di, D. Yuan, J. Pang, W. Wei, M. Wu and M. Hong, *Angew. Chem. Int. Ed.*, 2021, **60**, 7547-7552.
19. M. Zhang, B. Li, Y. Li, Q. Wang, W. Zhang, B. Chen, S. Li, Y. Pan, X. You and J. Bai, *Chem. Commun.*, 2016, **52**, 7241-7244.
20. X. P. Fu, X. Y. Le, Y. H. Xiao, D. M. Zeng, K. A. Zhou, L. Huang, Y. L. Wang and Q. Y. Liu, *Inorg. Chem.*, 2023, **62**, 15031-15038.
21. J. Lee, C. Y. Chuah, J. Kim, Y. Kim, N. Ko, Y. Seo, K. Kim, T. H. Bae and E. Lee, *Angew. Chem. Int. Ed.*, 2018, **57**, 7869-7873.

22. W. Yuan, W. Wang, P. Cen, H. Zhou, X. Liu and B. Liu, *Inorg. Chem.*, 2023, **62**, 15110-15117.
23. Y. Zhang, W. Sun, B. Luan, J. Li, D. Luo, Y. Jiang, L. Wang and B. Chen, *Angew. Chem. Int. Ed.*, 2023, **62**, e202309925.
24. J. Wu, Y. Wang, J. P. Xue, D. Wu and J. Li, *Inorg. Chem.*, 2023, **62**, 19997-20004.
25. J. Gao, X. Qian, R. B. Lin, R. Krishna, H. Wu, W. Zhou and B. Chen, *Angew. Chem. Int. Ed.*, 2020, **59**, 4396-4400.
26. W. Z. S. C. Xiang, Jose M. Gallegos, Y. Liu and B. L. Chen, *J. Am. Chem. Soc.*, 2009, **131**, 12415-12419.
27. L. Liu, Z. Yao, Y. Ye, Y. Yang, Q. Lin, Z. Zhang, M. O'Keeffe and S. Xiang, *J. Am. Chem. Soc.*, 2020, **142**, 9258-9266.
28. J. Pei, H. M. Wen, X. W. Gu, Q. L. Qian, Y. Yang, Y. Cui, B. Li, B. Chen and G. Qian, *Angew. Chem. Int. Ed.*, 2021, **60**, 25068-25074.
29. Y. Ye, S. Xian, H. Cui, K. Tan, L. Gong, B. Liang, T. Pham, H. Pandey, R. Krishna, P. C. Lan, K. A. Forrest, B. Space, T. Thonhauser, J. Li and S. Ma, *J. Am. Chem. Soc.*, 2022, **144**, 1681-1689.
30. Y. Ye, Z. Ma, R. B. Lin, R. Krishna, W. Zhou, Q. Lin, Z. Zhang, S. Xiang and B. Chen, *J. Am. Chem. Soc.*, 2019, **141**, 4130-4136.
31. X. Rao, J. Cai, J. Yu, Y. He, C. Wu, W. Zhou, T. Yildirim, B. Chen and G. Qian, *Chem. Commun.*, 2013, **49**, 6719-6721.